Biomass Conversion and Biorefinery (2023) 13:7783–7795
https://doi.org/10.1007/s13399-021-01825-y

ORIGINAL ARTICLE

Green synthesis of microalgal biomass-silver nanoparticle composite showing antimicrobial activity and heterogenous catalysis of nitrophenol reduction

Sushree S. Priyadarshini[1,2] · Shradhanjali Sethi[1] · Shweta Rout[1] · Pravat Manjari Mishra[1] · Nilotpala Pradhan[1,2]

Received: 8 April 2021 / Revised: 14 July 2021 / Accepted: 26 July 2021 / Published online: 14 August 2021

Abstract

In this study, we have demonstrated an integrated approach for utilization of microalga *Scenedesmus* sp. for fabrication of catalytic and antimicrobial silver nanoparticle composite. The algal biomass was harvested from an open raceway pond of 30,000 L scale used for CO_2 sequestration. The dried biomass served as a green, nontoxic, reducing and immobilizing agent for synthesis of silver nanoparticles, producing biomass-silver nanoparticle composite. ICP-OES was used to monitor the uptake of silver ions by biomass and subsequent formation of nanoparticles. The composite was calcined at 400 °C to fix the nanoparticles and prevent fouling. The calcined biomass-silver nanoparticle (CB-AgNP) composite was characterized using FESEM-EDAX, XRD and TGA. The CB-AgNP composite was used for the first time, as a heterogenous catalyst for reduction of a prominent industrial pollutant, p-nitrophenol. The reduction was carried out in the presence of $NaBH_4$ in aqueous medium under ambient conditions. Batch experiments were conducted to evaluate the effect of calcination temperature, load of material and its reusability, on the catalytic efficiency of material. It was found that as low as 5 mg mL^{-1} CB-AgNP material reduced more than 80% and 95% of p-nitrophenol within 1 min and 15 min of exposure, respectively. Rate of PNP reduction was 0.60 mg L^{-1} min^{-1}. The composite was easily recovered and reused for continuous batches of p-nitrophenol reduction. The efficiency of catalysis decreased with ten cycles of reuse; however, with an intermittent overnight water wash, the material regained its catalytic activity. Furthermore, the CB-AgNP composite also possessed excellent antimicrobial activity against pathogenic microbes. Two strains each of gram + ve and gram − ve bacteria and three strains of pathogenic fungi were used in the antimicrobial studies using well diffusion method and it was found to be active against all the microbes. The CB-AgNP composite is a potential candidate for a reusable heterogenous catalyst for designing continuous flow system for remediation of industrial effluents rich in p-nitrophenol. Its efficacy against common pathogenic bacteria and fungi can be harnessed for simultaneous antimicrobial treatment of the water. Moreover, this antimicrobial property will further inhibit the biofouling and eventual clogging of the material used in a packed column when used for water treatment.

Keywords Microalgae · *Scenedesmus* · Silver nanoparticle · p-Nitrophenol · Heterogenous catalysis · Antimicrobial activity

Highlights
- *Scenedesmus* biomass used for green fabrication of biomass-silver nanoparticle composite (CB-AgNP)
- CB-AgNP used as reusable heterogenous catalyst for p-nitrophenol reduction with 95% reduction
- CB-AgNP reused for ten cycles of PNP reduction
- CB-AgNP possessed excellent antimicrobial activity against pathogenic bacteria and fungi

1 Introduction

Concern for environmental pollution has risen in parallel to the rapid progress in industrialisation, with air and water pollution particularly demanding immediate mitigation strategies. In this regard, nanotechnology provides tremendous

✉ Nilotpala Pradhan
npradhan@immt.res.in

[1] Environment and Sustainability Department, CSIR-Institute of Minerals and Materials Technology (CSIR-IMMT), Bhubaneswar 751013, Odisha, India

[2] Academy of Scientific and Innovation Research, CSIR-Institute of Minerals and Materials Technology (CSIR-IMMT), Bhubaneswar 751013, Odisha, India

opportunity in development of efficient tools for the elimination of diverse pollutants from the environment. Nanoparticles synthesized using biological entities such as plants, algae, fungi and bacteria are greener and cheaper alternative to chemical synthesis [1–4]. One of the fascinating sources for such nanoparticles is microalgae. Microalgae are unicellular, photosynthetic algae with remarkable capacity for CO_2 fixation [5]. They are renewable and sustainable source of biofuels, neutraceuticals, cosmetics and food ingredients [6]. In the past few years, microalgae have emerged as an eco-friendly source for green synthesis of various nanoparticles with potential application in environmental mitigation [7–9]. *Scenedesmus* is a common freshwater microalga. It has high biomass productivity as compared to other microalgae and is easy to grow [10–12]. Due to high efficiency in CO_2 capture, many reports show its utilisation for sequestration of gaseous CO_2 emitted by industries like coal-based power plants and steel industry [13–16]. Cell-free extracts and live biomass of *Scenedesmus* have been reported for nanoparticle synthesis [17, 18]. In the current investigation, we report for the first time *as-harvested* dry biomass of *Scenedesmus* for synthesis as well as immobilization of silver nanoparticles. Once synthesized, the silver nanoparticles adhered to the biomass which together formed a biomass-nanoparticle composite. Calcination of the composite led to the formation of a solid, robust and reusable material, named as the Calcined Biomass-AgNP (CB-AgNP) composite. The CB-AgNP composite was used for reduction of p-nitrophenol (PNP) in the presence of sodium borohydride ($NaBH_4$).

PNP is a common organic pollutant, widely present in effluents of industries like dye production, pharmaceutical industries, fertilizer industries, leather tanning units and agricultural runoffs. The permissible limits of PNP in the environment by different agencies like the United States EPA and the European Commission are 0.43 µM (60 ppb) and 0.72 nM (0.1 ppb), respectively [19]. A simple and fast remediation method of PNP-contaminated water is selective hydrogenation of PNP to p-aminophenol (PAP) by $NaBH_4$. However, the reaction is not thermodynamically feasible and requires a catalyst. In recent times, many metal and non-metal nanocatalysts have been reported for degradation of organic pollutants [20, 21]. Most metal nanocatalysts are based on gold and silver nanoparticles. Though these metal nanoparticles are high in catalytic efficiency, their fabrication generally undergoes a complex set of procedures and/or use of toxic solvents [22–24]. Therefore, the quest for alternative eco-friendly greener reducing agents is significant. Subsequently, many studies have reported use of plant and microbial extracts for synthesis of metal nanocatalysts for PNP reduction [21, 25–28]. However, most protocols involve additional setup such as photocatalytic stimulus along with the nanoparticles for efficient catalysis [20, 29, 30]. Furthermore, efficiency of a catalyst also depends on its recovery and reuse [31]. Many green synthesized metal nanoparticles have been reported with good reusability (Table 1). Numerous studies have utilised aqueous plant based extracts derived from leaves, stem, fruit etc. to synthesize efficient nanocatalysts for PNP reduction. Algal biomass or extracts couldbe cheap sources of green reducing agents, but there are very few reports on them. There are even fewer reports where efficient PNP reduction took place and almost no such study where recovery and reuse of nanocatalyst were possible [32–34].

The present study tackles these aspects with a simple and comparatively cheap method of producing biomass-nanoparticle composite, efficient reduction of PNP without requiring light or any other reagent and easy recovery of the catalyst for reuse. Algal biomass, which may be a by product or waste in algal CO_2 sequestration process, was used as the base material for formulation of the biomass-silver nanoparticle composite. The calcined composite was found to be an efficient catalyst in the reduction of p-nitrophenol to p-aminophenol in the presence of sodium borohydrate in liquid medium under ambient condition. The composite is also efficient in terms of time consumption. More than 95% of the reduction takes place within 15 min of exposure to the catalyst. Being in solid phase, the catalyst could be recovered and reused again and again. One of the major challenges with heterogenous catalyst is loss of efficiency upon prolonged reuse. The composite used in this study also had similar fate. However, it was observed that, with a simple overnight water wash, the composite regained about 20% of its original catalytic efficiency. Apart from being an efficient heterogenous catalyst, the composite also possessed excellent antimicrobial activity against pathogenic fungi and bacteria. Antimicrobial activity is an additional property of the material. We investigated the antimicrobial activity of the material and found it very efficient against both bacteria and fungi. Microbial strains used for the study comprised two gram positive bacteria, *Staphylococcus aureus* and *Streptococcus pyogenes*; two gram negative bacteria, *Vibrio cholerae* and *Escherichia coli*; and three fungal strains, *Penicillium citrinum*, *Aspergillus flavus* and *Candida albicans*. Its efficacy against common pathogenic bacteria and fungi can be harnessed for simultaneous antimicrobial treatment of the water. Moreover, this antimicrobial property will inhibit the biofouling and eventual clogging of the material used in a packed column when used for water treatment.

This study demonstrates an integrated approach for utilisation of biomass produced during CO_2 sequestration at large scale can be used for the development of reusable and antimicrobial biomass-silver nanoparticle composite for catalytic reduction of p-nitrophenol.

Table 1 Comparison of PNP reduction efficiency of Ag and Au nanocatalysts produced using different plant and algae materials

Reducing agent	Nanocatalyst (medium)	[PNP]	Effective catalyst concentration per L of PNP	Reusability	Reduction time	Antimicrobial activity	Ref
Plants							
Sterculia acuminata fruit extract	Ag (colloidal)	10^{-3} M (1 mM)	0.09 mg L^{-1}	No	22 min	-	[35]
Thymbra spicata leaf extract	Ag (colloidal)	278 ppm (2 mM)	2 mg per10 mL (200 mg L^{-1})	Yes	1 min	-	[36]
Euphorbia heterophylla leaf extract	Ag/TiO_2 (composite)	2.5 mM	7 mg per 25 mL (280 mg L^{-1})	Yes	2 min	-	[37]
Sapindus mukorossi fruit extract	Ag (colloidal)	0.16 mM	0.0128 mM (1.38 mg L^{-1})	No	13 min	Antibacterial	[38]
Lotus garcinii leaf extract	Ag/RGO/Fe_3O_4 (composite)	2.5 mM	5 mg per 25 mL (200 mg L^{-1})	Yes	3 min	-	[39]
Abutilon hirtum leaf extract	Ag/RGO (composite)	2.5 mM	7 mg per 25 mL (280 mg L^{-1})	Yes	3.6 min	-	[40]
Nypa fruticans fruit husk extract	Ag (colloidal)	0.1 mM	3 mg per 2.5 mL (1200 mg L^{-1})	Yes	9 min	Antibacterial	[41]
Waste tea leaves extract	Ag-Au (hydrosol)	10^{-4} M (0.1 mM)	20 µL per1.5 mL (13 mL L^{-1})	No	7 min	-	[42]
Apium graveolens leaf extract	Au (colloidal)	20 mM	7.5 µL per 20µL (375 mL L^{-1})	No	22 min	-	[43]
Apium graveolens stem extract	Au (colloidal)	20 mM	2.5 µL/20 μL^{-1} (125 mL L^{-1})	No	12 min	-	[43]
Lawsonia inermis leaves extract	Au (colloidal)	0.4 mM	250 µg mL^{-1} (2500 mg L^{-1})	No	180 min	-	[44]
Phaseolus vulgaris extract	Ag (colloidal)	0.69 g/L (4.9 mM)	0.0001 mg mL^{-1} (0.1 mg L^{-1})	Yes	24 min	Antibacterial	[45]
Terminalia bellerica kernel extract	Ag (colloidal)	1 mM	0.4 mg mL^{-1} (400 mg L^{-1})	No	60 min	-	[26]
Algae							
Lobophora variegata extract	Au (colloidal)	2 mM	0.035 mg mL^{-1} (35 mg L^{-1})	No	4 min	-	[46]
Padina tetrastromatica extract	Au (colloidal)	2 mM	0.035 mg mL^{-1} (35 mg L^{-1})	No	4 min	-	[47]
Turbinaria conoides extract	Au (colloidal)	2 mM	300 µL per 1.4 mL (0.3 mLL^{-1})	No	5 min	-	[27]
Sargassum tenerrimum extract	Au (colloidal)	2 mM	300 µL per 1.4 mL (0.3 mLL^{-1})	No	5 min	-	[27]
Chlorella vulgaris powder	Au (colloidal)	2 mM	50 µL per 200 µL (0.25 mL L^{-1})	No	114 min	-	[28]
Arthrospira platensis (spirulina) powder	Au (colloidal)	2 mM	50 µL per 200 µL (0.25 mL L^{-1})	No	44 min	-	[28]

Table 1 (continued)

Reducing agent	Nanocatalyst (medium)	[PNP]	Effective catalyst concentration per L of PNP	Reusability	Reduction time	Antimicrobial activity	Ref
Scenedesmus biomass	Ag-biomass (composite)	10 ppm (0.072 mM)	5 mg of composite mL^{-1} (5000 mg of composite L^{-1} or 765 mg Ag per L	Yes	1 min (80%), 15 min (95%)	Antibacterial, antifungal	This work

2 Materials and methods

2.1 Chemicals

The chemicals used in this study were procured from HiMedia Pvt Ltd., India, and were of analytical grade. These were sodium hydroxide (NaOH), silver nitrate ($AgNO_3$), sodium borohydride ($NaBH_4$) and p-nitrophenol (PNP). Urea (46:0:0) and N:P:K (10:26:26) were procured from Indian Farmers Fertilizers Cooperative Limited (IFFCO), India, and Paradeep Phosphate Limited (PPL), India, respectively. All chemicals used in composite synthesis and application are of AR grade. While for growth of microalgae, commercial fertilizer in tap water was used as it was a large-scale open raceway pond experiment. All are generally used chemicals.

2.2 Synthesis of biomass-silver nanoparticle composite material

Microalga *Scenedesmus* sp. (IMMTCC-25) was cultivated in an open raceway pond of CSIR-IMMT under sunlight using low-cost media (0.1 gL^{-1} urea and 0.75 gL^{-1} NPK) with 0.0075 M NaOH for the purpose of CO_2 gas sequestration. The raceway pond was run at 30,000 L capacity. The CO_2 gas (20% mixed with air) was infused through the algal culture and NaOH was used as intermediate CO_2 sequester in medium. Later the algae utilised this CO_2 for photosynthetic growth in the raceway pond, thereby converting it into biomass. The biomass generated was a byproduct (or waste) of the microalgal CO_2 sequestration process. The biomass was harvested after 15 days of cultivation, dried under sunlight and stored until further use.

For the synthesis of silver nanoparticles, 1 M stock solution of silver nitrate ($AgNO_3$) was prepared in deionised water. About 10 g dry algal biomass was soaked overnight in 100 mL deionised water. The soaked biomass was washed twice and resuspended in 1 L deionised water. The stock solution of $AgNO_3$ was added to the biomass to obtain a final concentration of 10 mM $AgNO_3$. The suspension was kept at room temperature under constant stirring for 72 h. To monitor the bio-reduction of silver ions, 5 mL aliquot of the reaction solution was sampled at regular time intervals. The concentration of silver in the supernatant was analysed by inductively coupled plasma-optical emission spectrometry (ICP-OES; Perkin Elmer Optima 2100 DV) after appropriate dilution of the sample. In the control experiment, $AgNO_3$ was not added. Experiments were carried out in triplicates. After completion of the reaction, biomass was separated by filtration, washed with deionised water to remove unbound silver ions, if any, and dried in a hot air oven at 50 °C. The dried AgNP-bound biomass material (biomass-AgNP) was used for further studies. The AgNPs were fixed onto the biomass by subjecting the material to calcination in a muffle furnace at different temperatures.

2.3 Characterisation of biomass-AgNP material

Characterization is one of the major challenges during formulation of a heterogenous catalyst. As the AgNPs were embedded on the biomass, its direct quantification was not possible. Instead, ICP-OES was used to quantify Ag^+ ions in the synthesis medium as described in the previous section. The morphology and elemental composition of the biomass-AgNP complex were determined using FESEM-EDS. The thermal stability and weight loss pattern of the material was analysed using TGA-DTA. XRD was used to determine the phases of Ag present on the biomass. The moisture and ash content of the $AgNO_3$-exposed and unexposed biomass was also determined. The details of characterisation methodology are described below.

Field emission-scanning electron microscopy (FESEM; Carl Zeiss, Supra Gemini55) images of $AgNO_3$-exposed biomass were obtained to observe the morphology of the cells and the formation of AgNPs. The elemental composition of the sample was determined by EDS attached to the FESEM. Thermogravimetric analysis (TGA) was performed using a thermogravimetric-differential thermal analyzer (Mettler Toledo, TGA SDTA 851e). About 15–20 mg of $AgNO_3$-exposed biomass was heated to 1000 °C at the rate of 10 °C min^{-1} in aluminium oxide crucibles under nitrogen (99.9 wt% purity) atmosphere. X-ray diffraction (XRD) was carried out using an X-ray diffractometer (Panalytical, X'Pert Pro) having CuKα ($k = 1.54$ Å) radiation and a programmable divergence slit. AgNP-biomass materials calcined at different temperatures were used for the analysis. The moisture and ash content of the unexposed dry

biomass, uncalcined $AgNO_3$-exposed biomass and calcined $AgNO_3$-exposed biomass were analysed.

2.4 Reduction of p-nitrophenol

To a solution of 10 ppm (0.072 mM) p-nitrophenol, 5 mM sodium borohydride was added in the ratio 1:0.1 to form a yellow solution of p-nitrophenolate. CB-AgNP composite was added to the solution and stirred constantly for 15 min with a magnetic stirrer. Absorbance was measured at regular intervals using a UV–Visible spectrophotometer (Cecil 7400) between 300 to 600 nm. As the CB-AgNP particles remained suspended throughout the solution, they were first removed by centrifugation and the supernatant (which contained the PNP solution/reduction products) was used for accurate absorbance measurement. For this, 1 mL solution was sampled out at regular time intervals and centrifuged at 6000 rpm for 1 min. Centrifugation was done before every UV–Visible measurement in all further experiments in the study.

2.4.1 Optimization of catalyst load

To optimize the amount of CB-AgNP required for catalysis, the above reaction was carried out in batches using different amounts of CB-AgNP ranging from 1 to 8 mg mL^{-1}. PNP reduction was analysed using a UV–Visible spectrophotometer.

2.4.2 Optimization of calcination temperature

Calcination was necessary to fix the AgNPs on the biomass as well as prevent the fouling of the material during long-term storage. However, calcination is an energy- and time-intensive process. Determining an optimum calcination condition was necessary without compromising the catalytic output of the composite. Therefore, batches of CB-AgNP were calcined at different temperatures and then used for PNP reduction as above. Two grams of material were calcined at temperatures of 200 °C, 300 °C, 400 °C, 500 °C and 600 °C.

2.4.3 Recovery and reuse of catalyst

Reusability of the material was evaluated for 10 continuous cycles of reduction reactions. For this, the CB-AgNP material was recovered after each cycle of reduction by centrifugation and washed with distilled water before using in the next cycle. In another study of reuse, the material was kept suspended overnight in distilled water after five continuous cycles and then reused for additional five cycles.

All results were interpreted with respect to the percentage of PNP reduced within 15 min of reaction.

2.5 Antimicrobial tests

The antimicrobial activity of the CB-AgNP material was determined using well diffusion method. Six pathogenic microorganisms were used, viz. two gram positive bacteria, *Staphylococcus aureus* and *Streptococcus pyogenes*; two gram negative bacteria, *Vibrio cholerae* and *Escherichia coli*; and three fungal strains, *Penicillium citrinum, Aspergillus flavus* and *Candida albicans*. Nutrient agar plates and potato dextrose agar plates were used for bacteria and fungi, respectively. Plates were inoculated with small amount of respective microorganisms using spread plate technique. Three wells were punched in each plate using sterile tips. The CB-AgNP material was added in three different amounts in each plate, i.e. 10 mg, 20 mg and 50 mg. After incubation for 24 h, diameter of the inhibition zone was measured.

3 Result and discussion

3.1 Synthesis and characterisation of the CB-AgNP composite

For this study, the microalgal biomass generated as waste or byproduct during microalgal CO_2 sequestration process was used. Biomass was obtained after large-scale 30,000 L cultivation in an open raceway pond under sunlight. *Scenedesmus* biomass was harvested, dried and stored under room temperature. Throughout the storage period, the biomass retained its green colour. When exposed to silver nitrate solution, the colour of biomass changed from green to brown. This might be due to the conversion of Ag^+ ions to Ag^0 within the biomass. The control solution that did not have silver nitrate showed no visible colour change. Also while recovering the exposed biomass by filtration, the filtrate appeared colourless further suggesting that AgNPs were immobilised on the biomass. The same was confirmed by FESEM and XRD. As the AgNPs were surface-bound, the detailed mechanism of their formation is difficult to decipher. However, previous literature has shown that biomolecules present on the biomass are generally responsible for the reduction of $AgNO_3$ to AgNPs [18].

ICP-OES study of the filtrate showed that uptake of Ag^+ ions by the biomass was instantaneous. About 85% of Ag^+ ions were taken up by the biomass within 5 min of addition, after which Ag^+ concentration in the solution remained constant in the solution (Fig. 1a). However, a gradual change in colour of the biomass from green to brown was observed between 48 and 72 h of exposure. This indicated that while Ag^+ ions were adsorbed onto the biomass surface instantaneously, the formation of Ag^0 within the biomass was a gradual and slow process. In a similar study of the synthesis

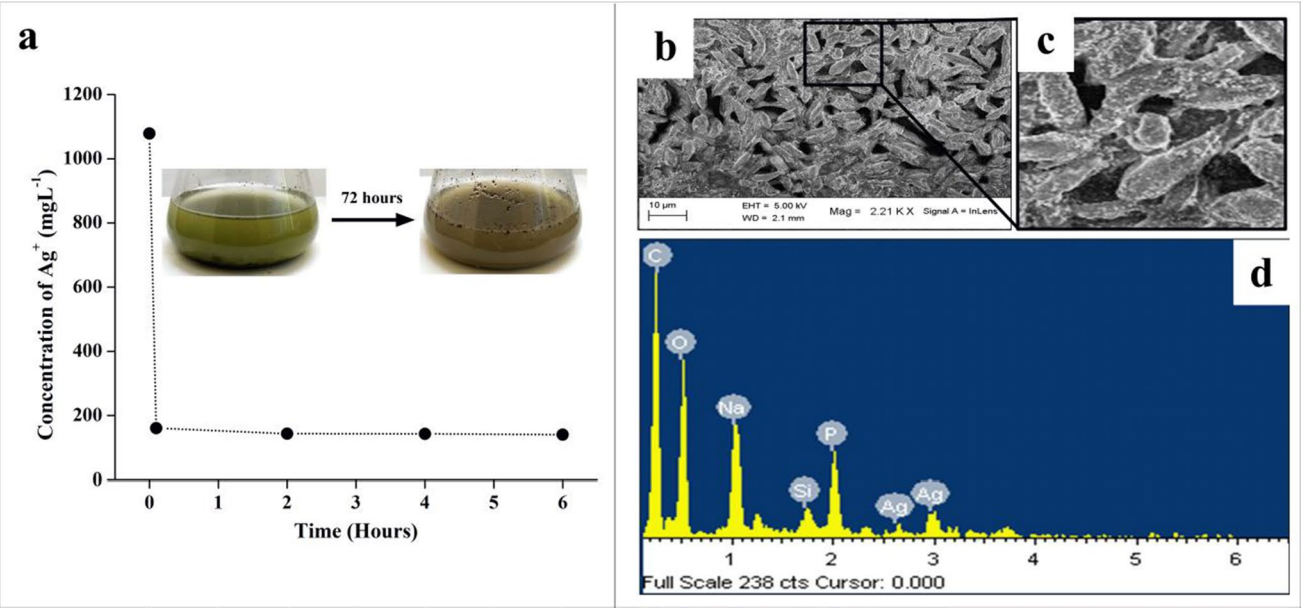

Fig. 1 **a** Change in concentration of Ag^+ ions in the reaction solution with respect to time of exposure as determined by ICP-OES; inset shows the optical image of biomass solution before and after synthesis of silver nanoparticles. FESEM micrograph: **b** and **c** show intact and broken cells of *Scenedesmus* with white spots representing silver nanoparticles. **d** EDS spectrum of the biomass

of silver nanoparticles using live *Scenedesmus* biomass culture, exposure time was optimised to 72 h [18].

FESEM micrograph (Fig. 1b, c) of the $AgNO_3$-exposed biomass showed the formation of silver nanoparticles. It revealed that most of the cells were still intact retaining their oval shape and measured roughly 10 µm. White spots on the cells represented AgNPs, distributed throughout the cell. EDS of typical biomass-AgNP composite showed signals for silver with additional peaks of C, O, Na, Si and P (Fig. 1d). The ash content analysis showed the presence of ash as high as 41.19% in the unexposed biomass. As the biomass was cultured in an open raceway pond, this could be due to dust entering in the medium and ultimately landing onto the biomass. As expected, the moisture content of the calcined $AgNO_3$-exposed biomass was lower and ash content was higher than its uncalcined counterpart (Table 2).

Since calcination is an important aspect of developing the CB-AgNP catalyst, determination of its thermal stability was vital. TGA-DTA of $AgNO_3$-exposed biomass showed the characteristic pattern of weight loss for *Scenedesmus* biomass (Fig. 2a). Corresponding to the pattern previously reported by Jena et al. [18], three stages of weight loss were observed. Initial weight loss below 200 °C may be assigned to the evaporation of free and bound water molecules. The second stage of weight loss observed between 200 and 400 °C may be assigned to decomposition of proteins and carbohydrates. In the final stage, decomposition of organic matter occurs beyond 400 °C. Maximum weight loss was observed in the first stage owing to high moisture.

Table 2 Moisture and ash content in $AgNO_3$ unexposed, exposed and calcined biomass

Sample	Moisture (%)	Ash (%)
Unexposed biomass	17.20	41.19
Silver exposed biomass	17.59	45.62
Calcined silver exposed biomass	2.37	96.51

Broadening of the second peak could be due to alteration in thermal stability of proteins due to binding of silver nanoparticles. In the third stage, weight loss was observed which prolonged from 600 °C until 750 °C. This may be due to silver nanoparticles resisting weight loss at higher temperatures as metals are known to have a slower rate of weight loss. Dust particles present in biomass (due to open raceway pond cultivation) also resist weight loss and may also be another contributing factor in the same. Also, weight loss at the third stage was lower than at the other stages.

XRD of the biomass-AgNP material revealed the nature of uncalcined ($AgNO_3$-exposed dried biomass) and calcined composite (Fig. 2b). The XRD peaks appeared more prominent with an increase in calcination temperature. The spectrum of the calcined materials, especially when calcined at 400 °C or above, showed Bragg reflection peaks at $2\theta = 38.48°$, 44°, 64.74° and 77.4°. These peaks correspond to the fcc structure of the AgNPs at lattice planes of (111), (200), (220) and (311). For signal peaks to be distinct in the XRD spectrum, the analyte

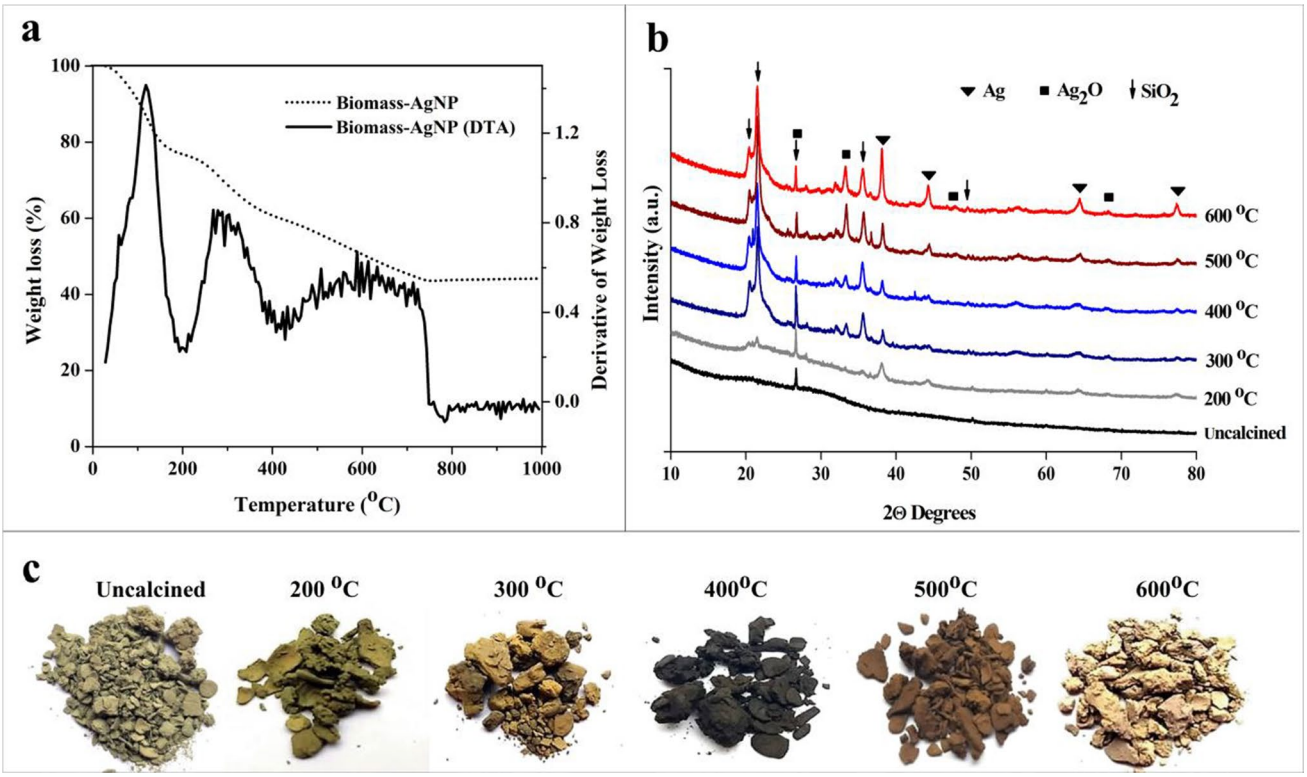

Fig. 2 **a** TGA-DTA of $AgNO_3$-exposed biomass. **b** XRD pattern of $AgNO_3$-exposed biomass calcined at different temperatures. **c** Respective optical images of materials

must constitute at least 5% of the sample. The revelation of the Ag peaks in materials calcined at higher temperatures was supportive of the above fact. Calcination led to the decomposition, oxidation and loss of organic content of the biomass, as evident from the TGA data, which increased the relative amount of metallic AgNPs in the sample. So as the temperature of calcination increased, diffraction peaks became more prominent. Additional peaks were those of Ag_2O, resulting out of oxidation of Ag within the material. Another high-intensity peak observed was that of SiO_2. Though small amount of Si is necessary for microalgal growth, presence of high amount of it could be attributed to silicates of dust particles getting into biomass as it was cultivated in an open raceway pond. The optical images of the calcined materials showed change in colour with increasing calcination temperature (Fig. 2c). The initial green colour of the biomass disappeared with gradual decomposition of chlorophyll pigments. As the temperature reached 400 °C, the biomass turned black due to charring. Further heating led to reduction of the biomass to a lighter coloured ash.

3.2 Reduction of p-nitrophenol and effect of CB-AgNP catalyst load

The catalytic efficiency of CB-AgNP was evaluated in the reduction of PNP in the presence of $NaBH_4$ as reducing agent. The reduction reaction generally takes place in two steps. In the first step, PNP is converted to p-nitrophenolate (PNP^-) ion by the addition of $NaBH_4$. This reaction is spontaneous and can be observed visually as the straw yellow colour of PNP solution changes to a bright yellow PNP^- solution. In the next step, hydrogenation of PNP^- takes place to form a colourless solution of PAP. However, this reaction is thermodynamically unfavorable and requires a suitable catalyst. The catalyst relays the electrons from BH_4^- to PNP^- and reduces the later to p-aminophenolate (PAP). A solution of PAP is colourless. Silver nanoparticles (AgNPs) were used as a catalyst by Pradhan et al. [48] for reduction of PNP where it was shown that small silver nanoparticles acted as nanoelectrodes efficiently transmitting electrons from BH_4^- for reduction of PNP to PAP [48]. While working with a heterogeneous catalysis system, many reports have proposed a four-step process for catalysis of

$NaBH_4$-mediated reduction of PNP [23, 49, 50]. Kong et al. [50] have provided further insights into the mechanism of the reduction process.

In the present study, when $NaBH_4$ was added to the PNP solution, an alkaline condition prevailed and PNP was converted to p-nitrophenolate (PNP^-). This reaction was observed visually as the straw yellow colour of PNP solution changed to a bright yellow PNP^- solution. PNP^- had an absorption maxima at 400 nm, as observed with UV–Visible spectroscopy. The catalytic efficiency of the material was depicted in terms of percentage of PNP reduction given by the formula $\frac{(Ci-Cf)}{Ci} \times 100$, where C_i and C_f are the initial and final concentration of PNP, respectively. Initial screening showed that *Scenedesmus* biomass alone had no catalytic activity as such while the CB-AgNP composite could catalyse the reduction of 80% of PNP^- within 1 min of addition (Fig. 3b). When left under constant stirring, more than 90% reduction was achieved within 15 min. The progress of the reaction was monitored by using UV–Visible spectroscopy (Fig. 3a). As the reaction advanced, the characteristic peak of PNP^- at 400 nm decreased while at around 300 nm a new peak appeared. This peak corresponded to PAP. The yellow colour of the solution faded gradually and completely bleached at the end of the reaction (Fig. 3c).

The amount of Ag^+ ions adsorbed by the biomass during synthesis was about 918 mg per 10 g of biomass. The concentration of Ag was 91.8 mg g^{-1} of biomass before calcination. After calcination at 400 °C, 40% weight loss was observed in the biomass and the Ag content of the CB-AgNP composite was 153 mg $g^{-1}$of composite. The optimum concentration of CB-AgNP used for PNP reduction was found to be 5 g L^{-1} which contained about 765 mg Ag L^{-1}.

The PNP reduction was carried out with different loads of the catalyst composite ranging from 1 to 8 mg mL^{-1}. Even with as low as 1 mg mL^{-1} of CB-AgNP, more than 50% reduction was observed. Evidently, with an increase in the load of CB-AgNP material from 1 to 8 mg mL^{-1}, efficiency of the catalyst increased up to 5 mg mL^{-1} and remained almost constant thereof (Fig. 4b).

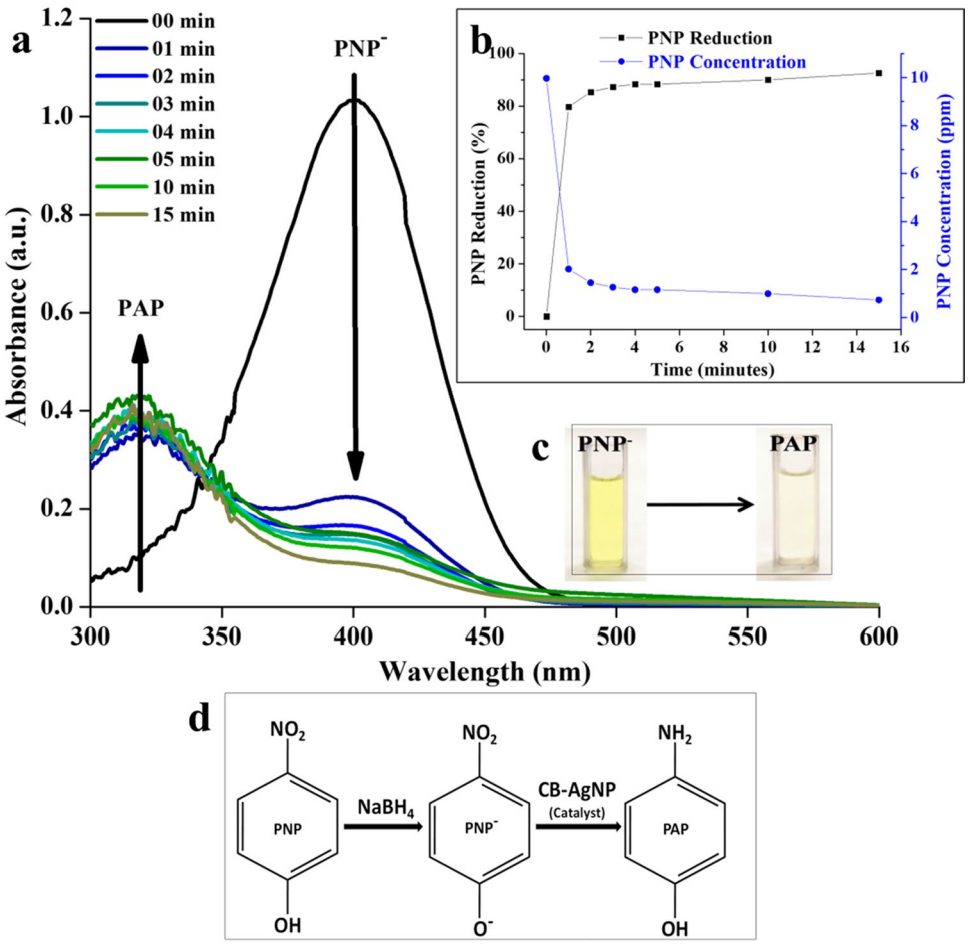

Fig. 3 **a** UV–Visible spectra of PNP^- reduction with CB-AgNP. **b** Percentage reduction vs. time of reaction. **c** Fading of yellow colour of PNP^- to a colourless PAP solution after reduction. **d** The reduction reaction of PNP to PAP by $NaBH_4$ in presence of CB-AgNP

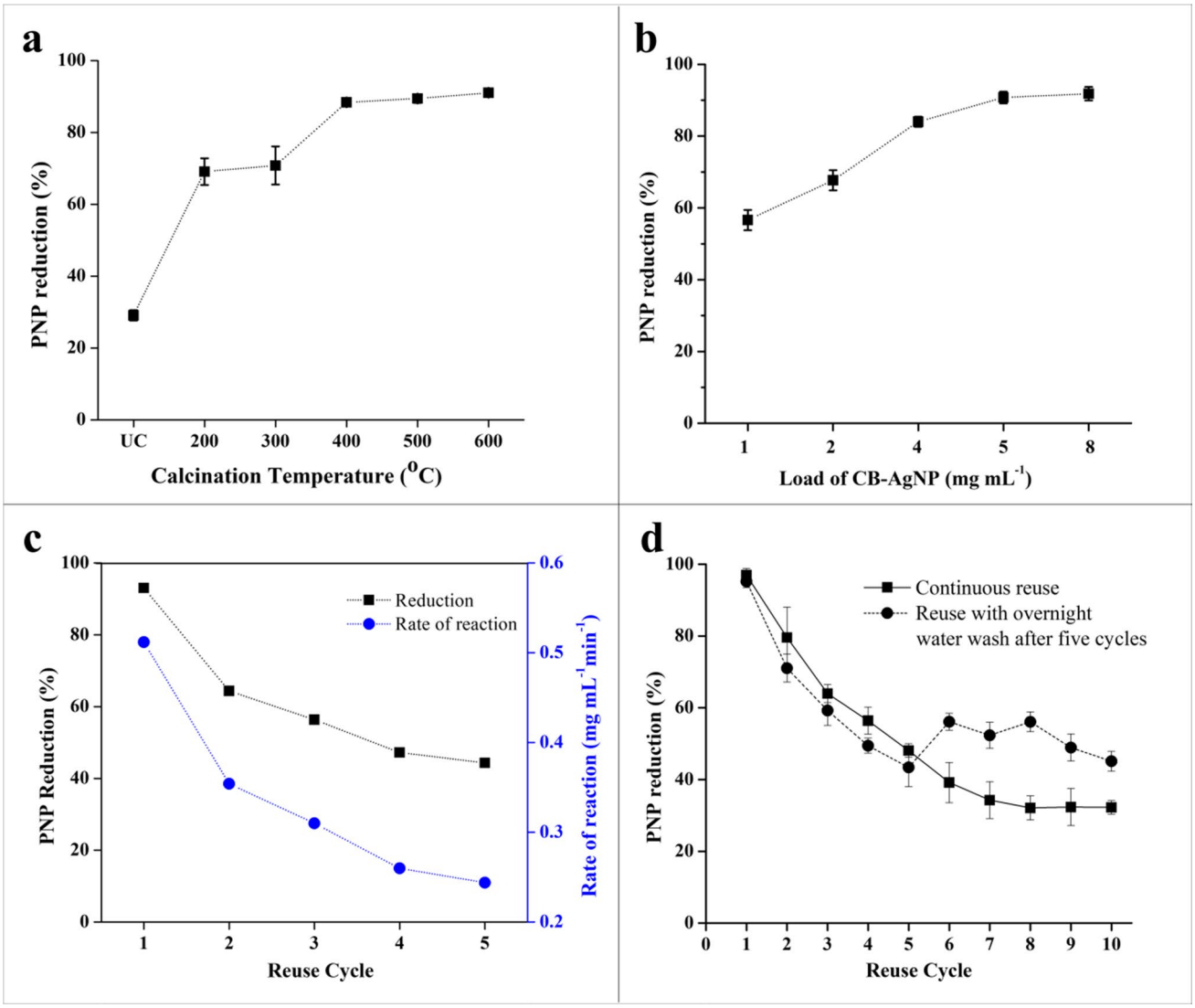

Fig. 4 Catalytic efficiency of CB-AgNP material with respect to **a** temperature of calcination and **b** load of the CB-AgNP material. **c** Reuse for five cycles. **d** Reuse for ten cycles with intermittent water wash

3.3 Effect of calcination temperature on the catalytic efficiency of CB-AgNP composite

Calcination was an important step in developing the CB-AgNP composite material as a catalyst. It fixed the AgNPs onto the biomass and prevented its decaying due to presence of moisture. To understand how calcination affected the catalytic activity of the material, batch experiments were carried out while varying the calcination temperature. As calcination is an energy-consuming process, these experiments helped in determining an optimum temperature (as low as possible) for calcination so as to ensure maximum catalytic efficiency while conserving as much energy as possible. Effect of calcination temperature on the percentage of PNP reduction was analysed (Fig. 4a). The uncalcined biomass showed poor catalytic activity probably due to the covering of biomaterials on the AgNPs making the reaction slower. It could reduce only about 30% PNP in the solution. With calcination, a significant increase in catalytic activity was observed. The CB-AgNP calcined at 200 and 300 °C reduced about 70% of PNP. With an increase in calcination temperature further to 400 °C, 90% PNP was reduced. Thereafter, a plateau of PNP reduction was observed up to temperature of 600 °C. FESEM micrograph showed that AgNPs were bound to cellular scaffolds in the biomass which were thermally stable until 600 °C (as observed in TGA). Calcining the material beyond it led to the decomposition of scaffolds, causing aggregation and fusion of silver nanoparticles, as evident from TGA-DTA data. Beyond that

temperature, decline in the catalytic efficiency of the material was observed. As higher temperature requires higher energy inputs, 400 °C was considered optimum and for all further experiments CB-AgNP material calcined at 400 °C was used (Fig. 4b).

3.4 Reusability of the CB-AgNP composite and rate of PNP reduction

The advantage of heterogeneous catalysis is its reusability. Hence, the reusability of the CB-AgNP material in PNP reduction was also evaluated (Fig. 4c and d). The material calcined at 400 °C was used for this study. When 5 mg mL^{-1} of the material was used for ten cycles of reactions continuously, PNP reduction declined gradually with each cycle. In the first cycle, the percentage of PNP reduced was as high as 95%, but it fell significantly to 40% by the sixth cycle. In another set of experiment, the material was used for five cycles of reduction, left suspended in distilled water overnight and reused again for another five cycles. Again PNP reduction declined gradually to around 45% in the first five cycles. Interestingly, when it was reused after overnight suspension in water, the catalytic activity of the material seemed to have recovered and PNP reduction increased to 60%. One of the important steps in heterogeneous catalysis is the adsorption of the substrates on to the catalyst surface. In the present case, p-nitrophenolate and BH_4^- might be getting adsorbed on to the CB-AgNP surface and diffused to the catalytic sites where AgNPs facilitated the transfer of electrons from BH_4^- to p-nitrophenolate, simultaneously reducing it to the final product, p-aminophenol (PAP). PAP molecules then get desorbed from the CB-AgNP surface and released into the solution. The efficacy of the material depended on the availability of surface area for PNP^- molecules to be adsorbed which subsequently depended on the removal of p-aminophenol molecules from the surface. The decrease in PNP reduction may be attributed to the loss of AgNPs in between cycles and/or the blockage of biomass surface and its catalytic sites by p-aminophenol molecules. The later phenomenon explains the recovery of the catalytic property of the material when subjected to an overnight water wash. Suspending the material in water might have facilitated the removal of p-aminophenol from the surface. However, the material recovered only to degrade 60% of PNP as opposed to 95% at the beginning, which might be due to the loss of AgNPs in between cycles/washing with water.

In this study, the reduction of PNP to PAP was monitored using UV–Visible spectroscopy. As the reaction took place in a heterogenous system, UV–Visible absorbance could only be measured after precipitating the composite catalyst powder from the solution using centrifugation. As reported, most of the reduction reaction (up to 80%) took place within the first 1 min of exposure of the composite to PNP solution. The batch mode experimental setup with freely suspended composite material in aqueous medium limited our capability to study the reaction within the first 1 min. The kinetics of PNP reduction in the reusability experiment is determined. Similarly, a gradual decline in the rate of reaction was observed for subsequent cycles of reduction. In the beginning, the rate of reaction was observed to be around 0.60 mg mL^{-1} min^{-1} which declined to 0.30 mg mL^{-1} min^{-1} at the fifth cycle. This observation was coherent with the decline in the percentage of PNP reduction to half of the initial value within five cycles of continuous reuse. If reused continuously without break, the rate further decreased to 0.20 mg mL^{-1} min^{-1} by completion of ten cycles. But with an intermittent water wash after five cycles, the rate of reaction increased in the sixth cycle to 0.35 mg mL^{-1} min^{-1} and remained at about 0.30 mg mL^{-1} min^{-1} after ten cycles. The decline in the rate of reaction suggests an adsorption-mediated catalysis process. A possible mechanism constituting four basic steps of the adsorption-mediated, CB-AgNP catalysed reduction of PNP to PAP is shown in Fig. 5.

A comparison between the catalytic efficiency of different noble metal nanocatalysts synthesized using plant and algal sources has been tabulated in Table 1. As evident, there are reports of many plant extract–based reusable and efficient nanocatalysts. However, algal sources are limited and most of them are derived from marine resources. Additionally, none of reported algal-based nanocatalysts are reusable.

3.5 Antimicrobial tests

The antimicrobial activity of the CB-AgNP material is illustrated in Fig. 6. Measurement of zone of inhibition (ZoI) shows that the material confers decent activity against both bacterial and fungal strains. The activity increased with increase in the material load in each microbial plate. At 10 mg load, the material showed comparable activity against all strains of microorganism. However, as the material load was increased to 50 mg, distinctive activity was observed against fungal strains. The ZoI measurements are shown in Table 3.

The mechanism by which AgNPs confer molecular toxicity remains highly debated to date. Some authors report particle-specific activity of silver nanoparticles where the size, shape and surface charge and functional ligands on the nanoparticles are said to be the responsible factors [51]. Whereas other reports sustain that release of silver ions from the nanoparticle core upon oxidation is necessary for their antimicrobial activity [52]. In this study, the silver nanoparticles remain bound to *Scenedesmus* biomass and XRD pattern shows the presence of both metallic and oxidized Ag. Though the material was found to be an

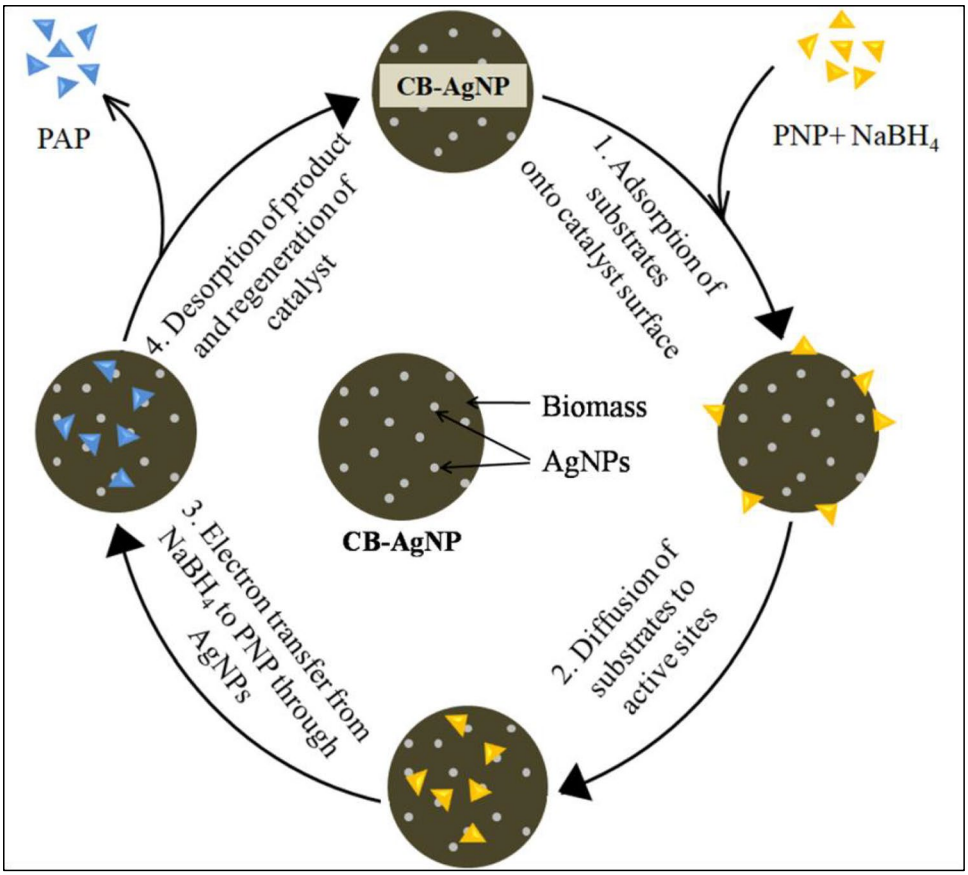

Fig. 5 Possible mechanism of PNP reduction by $NaBH_4$ in presence of CB-AgNP material

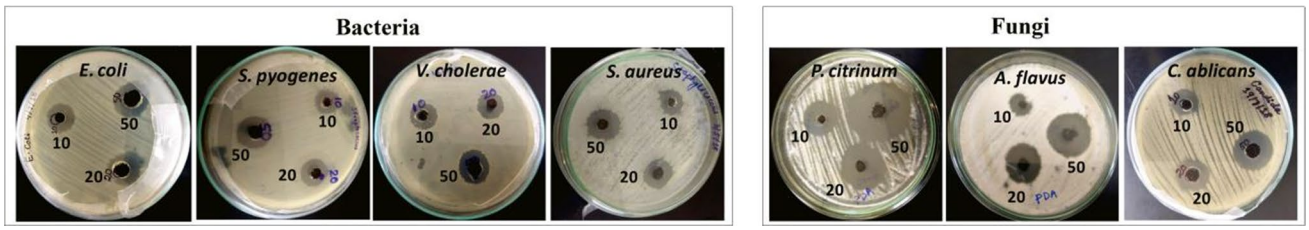

Fig. 6 Agar diffusion method showing zone of inhibitions of bacteria and fungi growth in presence of different loads of CB-AgNP material

Table 3 Zone of inhibition of antimicrobial tests using CB-AgNP material

Microbial strain		Inhibition zone (cm)		
		CB-AgNP (10 mg)	CB-AgNP (20 mg)	CB-AgNP (50 mg)
Gram – ve Bacteria	*Escherichia coli*	1.72 ± 0.05	1.85 ± 0.17	1.97 ± 0.12
	Vibrio cholerae	1.42 ± 0.05	1.45 ± 0.06	1.72 ± 0.09
Gram + ve Bacteria	*Streptococcus pyogenes*	1.35 ± 0.06	1.45 ± 0.06	1.82 ± 0.05
	Staphylococcus aureus	1.48 ± 0.05	1.52 ± 0.05	1.95 ± 0.06
Fungi	*Penicillium citrinum*	2.27 ± 0.09	2.62 ± 0.05	3.20 ± 0.12
	Aspergillus flavus	1.32 ± 0.10	2.17 ± 0.05	2.92 ± 0.05
	Candida albicans	1.48 ± 0.09	1.84 ± 0.08	2.28 ± 0.04

efficient antimicrobial agent, it could not be determined whether AgNPs or Ag^+ ions were responsible for it.

4 Conclusion

We discovered that dry microalgae biomass harvested during CO_2 sequestration as waste of the process can be used to synthesize silver nanoparticles with catalytic and antimicrobial properties. The silver nanoparticle–immobilised biomass could efficiently catalyse the reduction of PNP in aqueous condition without requiring light or any other reagent. The composite could reduce 80% and 95% of PNP within 1 min and 15 min of exposure, respectively. As the CB-AgNP was a solid phase catalyst, it could be recovered and reused efficiently with intermittent breaks between consecutive cycles of reduction. A continuous system with CB-AgNP material packed column can be developed in the future for reduction of p-nitrophenol. The reduction and removal of p-nitrophenol hold both environmental and industrial significance. Hence, this material is an efficient and economic source for p-nitrophenol reduction. The material was also found to be a potent antimicrobial agent with activity against gram positive and gram negative bacteria as well as pathogenic fungi. Its efficacy against common pathogenic bacteria and fungi can be harnessed for simultaneous antimicrobial treatment of the water. Moreover, this antimicrobial property will inhibit the biofouling and eventual clogging of the material used in a packed column when used for water treatment. In the quest for development of novel antimicrobial products, the CB-AgNP composite can prove to be an efficient supplement in exterior coatings in buildings and establishments for maintaining an aseptic environment/topical applications. This study also demonstrates the potential of microalgae biomass-silver nanoparticle in the development of an eco-friendly and sustainable integrated system targeted towards CO_2 sequestration, industrial p-nitrophenol reduction and microbial disinfection.

Acknowledgements All authors are thankful to Director CSIR-IMMT, Bhubaneswar for permission to publish this article. NP would like to thank the financial support of Department of Science and Technology, Government of India (Grant Number DST/IS-STAC/CO_2-SR-169/13(G) and DST-UKIERI Award No. DST/INT/UK/P-128/2016). SSP would like to thank Council of Scientific and Industrial Research, Govt. of India for the fellowship under CSIR-JRF Scheme (Grant Number 20/12/2015 (ii) EU-V).

Declarations

Conflict of interest The authors declare no competing interests.

References

1. Gupta A, Tandon M, Kaur A (2020) Nanotechnol Environ Eng 5:27. https://doi.org/10.1007/s41204-020-00092-y
2. Shah M, Fawcett D, Sharma S, Tripathy SK, Poinern GEJ (2015) Materials (Basel) 8(11):7278–7308. https://doi.org/10.3390/ma8115377
3. Duan H, Wang D, Li Y (2015) Chem Soc Rev 44:5778–5792
4. Dahoumane SA, Mechouet M, Wijesekera K, Filipe CDM, Sicard C, Bazylinski D, Jeffryes C (2017) Green Chem 19:552–587
5. Khan MI, Shin JH, Kim JD (2018) Microb Cell Fact 17:36. https://doi.org/10.1186/s12934-018-0879-x
6. Das P, Aziz SS, Obbard J (2011) Two phase microalgae growth in the open system for enhanced lipid productivity. Renew Energy 36:2524–2528
7. Arsiya F, Sayadi MH, Sobhani S (2017) J Water Environ Nanotechnol 2(3):166–173
8. Jena J, Pradhan N, Aishvarya V, Nayak RR, Dash BP, Sukla LB, Panda PK, Mishra BK (2014) J Appl Phycol 27:2251–2260
9. Khanna P, Kaur A, Goyal D (2019) J Microbiol Methods 163:105656. https://doi.org/10.1016/j.mimet.2019.105656
10. Hanagata N, Takeuchi T, Fukuju Y, Barnes DJ, Karube I (1992) Phytochemistry 31(10):3345–3348. https://doi.org/10.1016/0031-9422(92)83682-O
11. Jena J, Nayak M, Panda HS, Pradhan N, Sarika C, P&a, P, Rao VSK, Prasad BN, Shukla LB (2012) World Environ 2(1), 11 - 16. https://doi.org/10.5923/J.ENV.20120201.03
12. Rhee G (1973) J Phycol 9:495–506. https://doi.org/10.1111/j.1529-8817.1973.tb04126.x
13. Basu S, Roy AS, Mohanty K, Ghoshal AK (2013) Bioresour Technol. 143:369–377. https://doi.org/10.1016/j.biortech.2013.06.010
14. Ho SH, Chen WM, Chang JS (2010) Bioresour Technol 101(22):8725–8730. https://doi.org/10.1016/j.biortech.2010.06.112
15. Nayak M, Rath SS, Thirunavoukkarasu M, Panda PK, Mishra BK, Mohanty RC (2013) J Microbiol Biotechnol 28(23(9)):1260–1268. https://doi.org/10.4014/jmb.1302.02044
16. Pradhan N, Das B (2018) Recent advancements in biofuels & bioenergy utilization. Springer, Singapore, pp 285–302
17. Aziz N, Fatma T, Varma A, Prasad R (2014). J Nanoparticles. https://doi.org/10.1155/2014/689419
18. Jena J, Pradhan N, Nayak R, Dash BP, Sukla LB, Panda PK, Mishra BK (2014) J Microbiol Biotechnol 24(4):522–533
19. Wei Y, Kong LT, Yang R, Wang L, Liu J, Huang X (2011) Langmuir 27(16):10295–10301. https://doi.org/10.1021/la201691c
20. Mortazavi-Derazkola S, Salavati-Niasari M, Amiri O, Abbasi A (2016). J Energy Chem. https://doi.org/10.1016/j.jechem.2016.10.015
21. Saim AK, Adu PCO, Amankwah RK, Oppong M, Darteh MN, Darteh FK, Mamudu AW (2021) Environ Technol Rev 10(1):111–130. https://doi.org/10.1080/21622515.2021.1893831
22. Chiou JR, Lai BH, Hsu KC, Chen DH (2013) J Hazard Mater 248–249:394–400. https://doi.org/10.1016/j.jhazmat.2013.01.030
23. Fang W, Deng Y, Tang L, Zeng G, Zhou Y, Xie X, Wang J, Wang Y, Wang J (2017) J Colloid Interface Sci 490:834–843
24. Ren ZH, Li HT, Gao Q, Wang H, Han B, Xia KS (2017) Mater Des 121:167–175. https://doi.org/10.1016/j.matdes.2017.02.064
25. Tavakoli F, Salavati-Niasari M, Babiei A, Mohandes F (2015) Mater Res Bull 63:51–57. https://doi.org/10.1016/j.materresbull.2014.11.045
26. Sohail SL, Amjad A, Mustafa U, Jabeen M, Ul-Hamid R A (2020) Colloid Interface Sci Commun 37:100276. https://doi.org/10.1016/j.colcom.2020.100276
27. Ramakrishna M, Rajesh Babu D, Gengan RM et al (2016) J Nanostruct Chem 6:1–13. https://doi.org/10.1007/s40097-015-0173-y

28. Zayadi RA, Bakar FA (2020) J Environ Chem Eng 8:103843. https://doi.org/10.1016/j.jece.2020.103843
29. Ahmed S, Rasul MG, Martens WN, Brown R, Hashib MA (2010) Desalination 261(1–2):3–18
30. Yang L, Luo S, Li Y, Xiao Y, Kang Q, Cai Q (2010) Environ Sci Technol 44(19):7641–7646
31. Beshkar F, Khojasteh H, Salavati-Niasari M (2017). J Colloid Interface Sci. https://doi.org/10.1016/j.jcis.2017.02.016
32. Francis S, Joseph S, Koshy EP, Mathew B (2017) Environ Sci Pollut Res Int 24(21):17347–17357. https://doi.org/10.1007/s11356-017-9329-2
33. Rajegaonkar PS, Deshpande BA, More MS, Waghmare SS, Sangawe VV, Inamdar A (2018) Mater Sci Eng C 93:623–629
34. Zhang W, Tan F, Wang W, Qiu X, Qiao X, Chen J (2012) J Hazard Mater 217–218:36–42
35. Bogireddy NKR, Kumar HAK, Mandal BadalKumar (2015) Journal of Environmental. Chem Eng. https://doi.org/10.1016/j.jece.2015.11.004
36. Veisi H, Azizi S, Mohammadi P (2017). J Clean Prod. https://doi.org/10.1016/j.jclepro.2017.09.265
37. Atarod M, Nasrollahzadeh M, Sajadi SM (2016) J Colloid Interface Sci 462:272–279. https://doi.org/10.1016/j.jcis.2015.09.073
38. Dinda G, Halder D, Mitra A, Pal N, Vasquez-Vasquez C, Atrura M (2017) New J Chem 41:10703–10711. https://doi.org/10.1039/C7NJ00704C
39. Maham M, Nasrollahzadeh M, Sajadi SM, Nekoei M (2017). J Colloid Interface Sci. https://doi.org/10.1016/j.jcis.2017.02.064
40. Maryami M, Nasrollahzadeh M, Mehdipour E, Sajadi SM (2016) Int J Hydrogen Energy 41(46):21236–21245
41. Doan V-D, Phung M-T (2020) Thi Lan-Huong Nguyen, Thanh-Chi Mai, Thanh-Danh Nguyen. Arab J Chem 13:7490–7503. https://doi.org/10.1016/j.arabjc.2020.08.024
42. Kang C-W, Kolya H (2021) Sustainability 13:3318. https://doi.org/10.3390/su13063318
43. Khoshnamvand M, Hao Z, Huo C et al (2020) Int J Environ Sci Technol 17:2433–2442. https://doi.org/10.1007/s13762-020-02632-0
44. Kumari P, Meena A (2020) Colloids Surf A: Physicochem Eng Asp 606:125447. https://doi.org/10.1016/j.colsurfa.2020.125447
45. Rani P, Kumar V, Singh PP, Matharu AS, Zhang W, Kim KH, Singh J, Rawat M (2020) Environ Int 143:105924. https://doi.org/10.1016/j.envint.2020.105924
46. Francis PK, Sivadasan S, Avarachan A, Gopinath A (2019). Part Sci Technol. https://doi.org/10.1080/02726351.2018.1547340
47. Princy KF (2019) Anu Gopinath Mater Today: Proc 9:38–45. https://doi.org/10.1016/j.matpr.2019.02.034
48. Pradhan N, Pal A, Pal T (2002) Colloids Surf A 196:247–257
49. Gupta VK, Atar N, Yola ML, Üstündağ Z, Uzun L (2014) Water Res 48:210–217
50. Guo P, Tang L, Tang J, Zeng G, Huang B, Dong H, Zhang Y, Zhou Y, Deng Y, Ma L, Tan S (2016) J Colloid Interface Sci 469:78–85
51. Duran N, Duran M, Jesus B, Seabra AB, Favaro WJ, Nakazato G (2016) Nanomedicine: Nanotechnol Biology Med 12:789–799
52. Xiu Z, Zhang Q, Puppala HL, Colvin VL, Alvarez JJ (2012) Nano Lett 12:4271–4275